6.6 ***LABORATORY EXPERIMENTS ON THE EFFECTS OF WIND DIRECTION ON BEHAVIOR OF FIRE WHIRLS DOWNWIND OF FIRE***

Masahiko Shinohara * and Sanae Matsushima
National Research Institute of Fire and Disaster, Tokyo, Japan

1. INTRODUCTION

Fire whirls cause destructive damage in and around large fires, such as wild fires and city fires. They are frequently observed downwind of fires in flat terrain, sometimes moving and sometimes stationary. However, there has been little investigation into the effects of the wind direction on the behavior of fire whirls.

The purposes of this study are to investigate the effects of wind direction on the behavior of fire whirls located downwind of a rectangular flame and the formation of fire whirls. The fire whirls studied here does not contain fire.

2. METHOD

2.1 *Experimental Apparatus*

The experiments were carried out using a 4-m-diameter fan located in a 25 × 25 × 22-m (*l* × *w* × *h*) laboratory environment. Figure 1 shows the experimental setup. Ten fuel pools with internal dimensions of 29.7 x 29.7 cm and a depth of 2.1 cm were placed in two rows such that they were in contact with each other and flush with the 5.46 × 5.46 × 1.55-m (*l* × *w* × *h*) horizontal artificial floor. The total area of the pools was 151 x 60 cm. Methanol was used as the fuel. The floor downwind of the pools was an 182.0 × 91.0 × 0.5-cm (*l* × *w* × *t*) transparent thermally resistant glass plate.

2.2 *Experimental Method*

We carried out two experiments. In the first, the wind direction was perpendicular to the long axis of the fuel pools; in the second, it was parallel to the long axis of the fuel pools. We placed 700 g of methanol in each fuel pool. The wind velocity was controlled using the fan and was measured using a hot-wire anemometer (Kanomax, Model

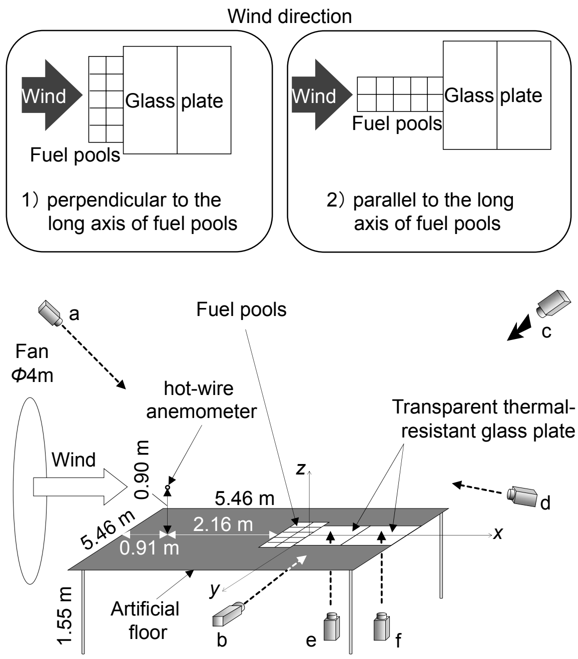

Figure 1. The experimental apparatus.

6162); the nominal velocity was constant, and the mean measured wind velocity was in the range $0.80 \leq U \leq 0.86$ m/s. Fire whirls and the airflow around the flame were visualized using a smoke-wire flow visualization technique, as the fire whirls considered here were air vortices. The wires were located above the glass plate at right angles to the wind direction and parallel to the floor, at x = 70 cm, z = 3 cm, and at x = 130 cm, z = 3 cm. Additional wires were located at both sides of and upwind of the fire source, at a height of 3 cm above the floor. For the experiment described in Section 3.3, an additional wire was located 80 cm above the floor upwind of the fire source. Six video cameras (labeled a–f in Figure 1) were used to capture images of the airflow around the flame.

To analyze the behavior of the fire whirls, the air entrainment velocity into the flame was measured under no-wind conditions using a hot-wire anemometer at x = 40 cm, y = 7 cm, z = 3 cm. The measurements were carried out with two arrangements of fuel pools, as shown in Figure 1. This allowed us to measure the velocity of air

* *Corresponding author address:* Masahiko Shinohara, Natl. Res. Inst. of Fire and Disaster, Tokyo 182-8508, Japan; e-mail: shino@fri.go.jp
11th Symposium on Fire and Forest Meteorology, 2015.

entrainment into the long and short sides of the fire source. The air temperature was also obtained using the anemometer. Two smoke wires were placed at right angles to the wind direction and parallel to the floor at x = 40 cm, $y \leq$ -7 cm, z = 3 cm, and at x = 100 cm, $y \leq$ -7 cm, z = 3 cm. In addition, the video cameras labeled e and f in Figure 1 were used to measure the entrainment velocity based on smoke movement.

The vertical profile of the wind velocity under no-flame conditions was measured at x = -273.4 cm and y = 0 cm.

2.3 *Analysis Method*

To discuss the motion of the vortices, the location of the vortices was measured using video images captured from underneath the glass plate downwind of fuel pools using video cameras e and f. The velocity field in the horizontal plane in vortices was measured based on the motion of smoke ejected from a smoke wire located at x = 70 cm, z = 3 cm using the video images captured by video camera e. The measurements were carried out when the center of the vortex was located on the wire.

3. RESULTS AND DISCUSSION

3.1 *Behavior of Fire Whirls*

The behavior of fire whirls vary considerably, depending on the wind direction, in spite of the same wind speed and the same heat release rate. When the wind direction was perpendicular to the long axis of the fire source, the fire whirls formed the almost stationary vortex pair, as shown in Figures 2(a) and 3(a). Figure 2(a)-a shows a top view of a vortex pair, and Figure 2(a)-e shows a view from beneath the glass plate. The direction of the airflow is from the bottom of the images to the top. The vortex located on the left side in the image in Figure 2(a)-a rotated clockwise, and the vortex located on the right side rotated counterclockwise. Figures 3(a) and 3(b) show the path of the vortices observed from beneath the glass plate downwind of the flame.

When the wind direction was parallel to the long axis of the fire source, fire whirls were shed downwind one by one, as shown in Figures 2(b) and 3(b). The mean shedding velocity of the fire whirls was 0.5 m/s for the data shown in Figure 3(b). This velocity was smaller than the wind velocity generated by the fan. This will be discussed further in Section 3.4.

(a)

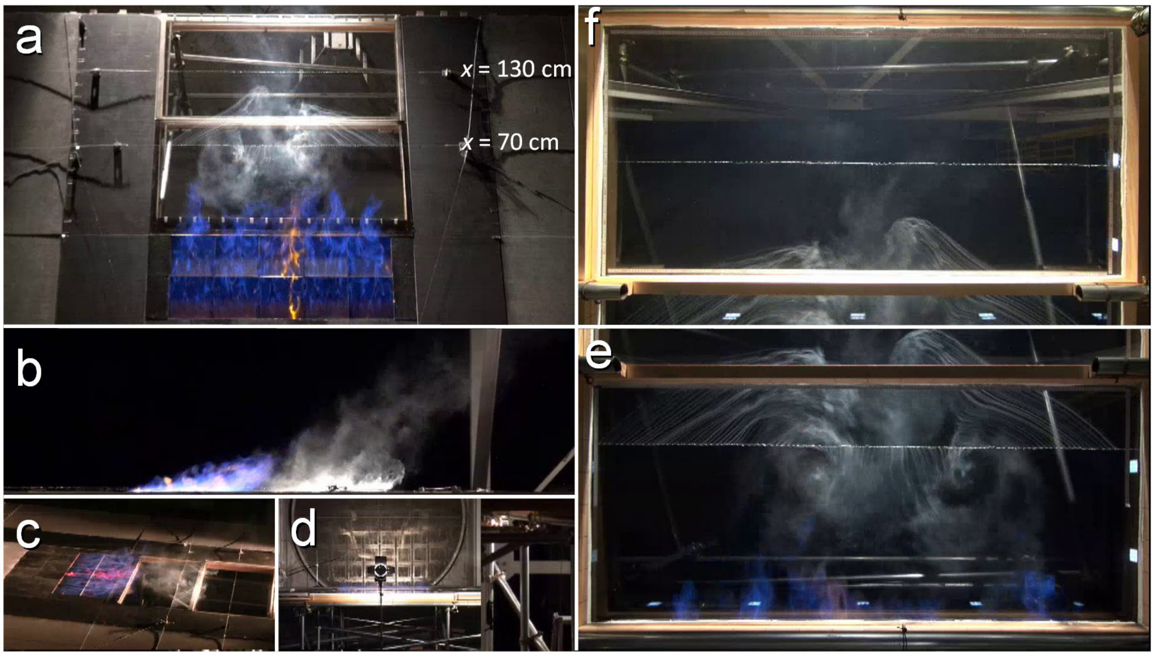

Figure 2. Fire whirls visualized with smoke. Images were captured using the video cameras labeled a–f in Figure 1. (a) With the wind direction perpendicular to the long axis of the fuel pools. (b) With the wind direction parallel to the long axis of the fuel pools.

(b)

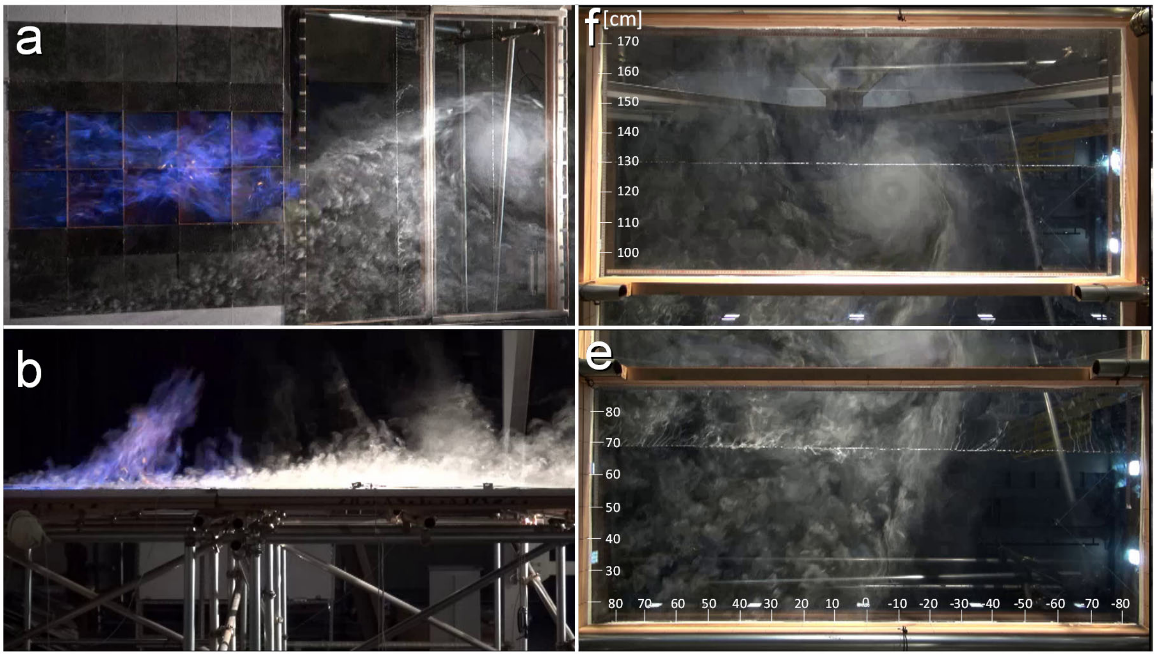

Figure 2. (*Continued*).

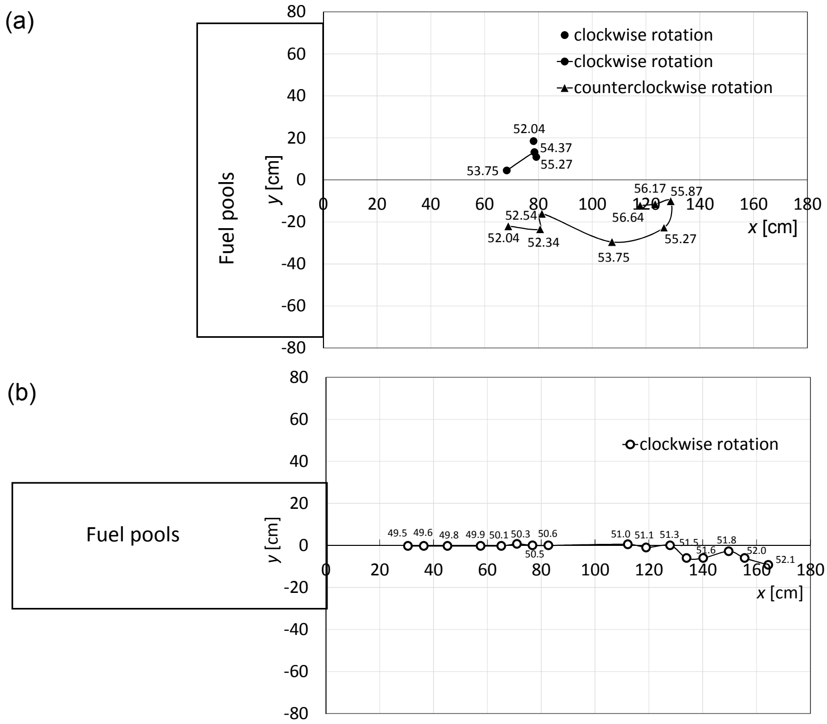

Figure 3. Example paths of the center of the fire whirls observed from beneath the glass plate downwind of the flame. The figures annotated by each symbol show the time from ignition in seconds. (a) With the wind direction perpendicular to the long axis of the fuel pools. (b) With the wind direction parallel to the long axis of the fuel pools.

3.2 ***Formation of Fire Whirls***

We investigated formation process of fire whirls when the wind direction was parallel to the long axis of the fire source using the video images.

One or two small vertical fire vortices appeared at the downwind side of a flame, as shown in Figure 4(a) and 4(b). When vortices appeared as a pair, they rotated in opposite directions. Smoke was injected 3 cm above the floor. When one of the rotating flames became larger than the other, the airflow downwind of the larger rotating flame was greater, and the airflow began to form a vortex v1 that rotated in the same direction as the larger rotating flame, as shown in Figures 5(a) and 6(a). This vortex was then shed, as shown in Figures 5(b) and Figure 6(b). On the other hand, the air vortex v2 that rotated in the opposite direction appeared to form where two airflows that passed both sides of the flame met, as shown in Figures 5(a) and 6(a). On some occasions the airflow rotated around the rotating flame. We were not able to identify whether the rotating flame led to the formation of the air vortex or the reverse. Moreover, we were unable to determine whether the observed location of the formation of the air vortices was the origin of these fire whirls.

(a)

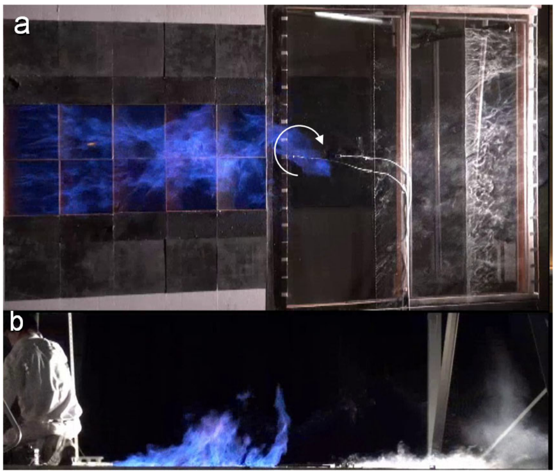

Figure 4 (a). Top and side views of a vertical fire vortex.

(b)

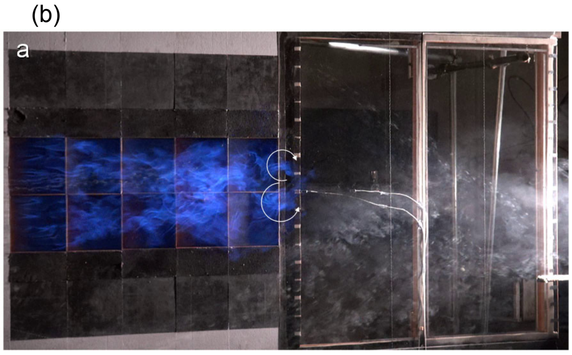

Figure 4 (b). Top view of a pair of vertical fire vortices. The wind direction was parallel to the long axis of the fuel pools.

(a)

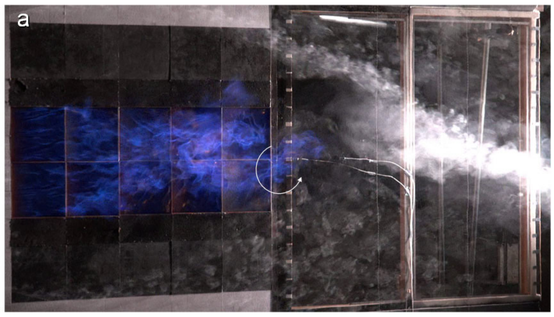

(b)

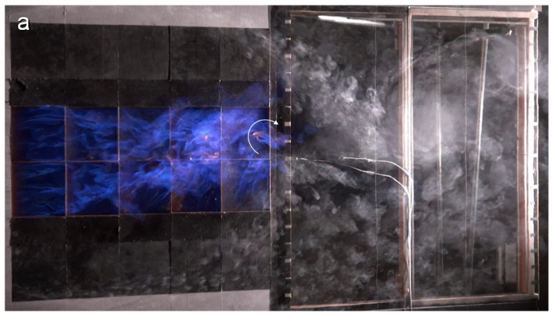

Figure 5. The formation process of fire whirls visualized with smoke. The wind direction was parallel to the long axis of the fuel pools.

(a) (b)

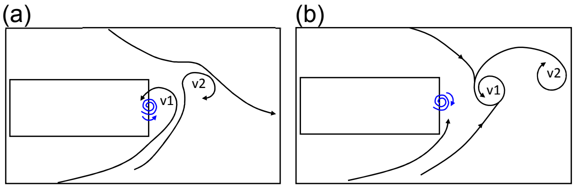

Figure 6. The formation process of fire whirls (v1, v2). The blue line shows a vertical fire vortex.

When the wind direction was perpendicular to the fire source, we were not able to observe the formation of fire whirls (i.e., vortex pairs). The fire whirls appeared to be the lower part of counter-rotating vortex pairs (CVPs) of the plume of the flame, as has been observed downwind of a small flame (Shinohara and Matsushima, 2012). However, fire whirls may be other vertical vortices, as has also been observed downwind of a small flame (Shinohara and Kudo, 2004, Shinohara and Matsushima, 2012).

The rotating flames appeared only when the wind direction was parallel to the long axis of the fire source. The flame shape shown in Figure 7 and the motion of the smoke shown in Figures 2(b), 5(a), 5(b) and 7 suggest that the wind at both sides of the flame near the floor entered both sides of the flame, as shown in Figure 8. However, when the wind direction was perpendicular to the long axis of the fire source, the wind near the floor appeared not to enter the side of the flame, as shown in Figures 9 and 10. This is because the airflow passing the long side of the fire was affected by entrainment of higher velocities into the flame for longer periods than was the case when the airflow passed the short side of the fire. If the origin of the rotating flames is located on both sides of the flame near the floor, as with the origin of CVPs in the plume, as was suggested by the experiments of Haines and Smith (1983) and the numerical simulations of Cunningham *et al*. (2005) and Shinohara (2010), then entrainment into the sides of the flame may cause the origin of the vortex to enter the flame, resulting in a rotating flame at the downwind side of the fire source only when the wind direction is parallel to the long axis of the fire source.

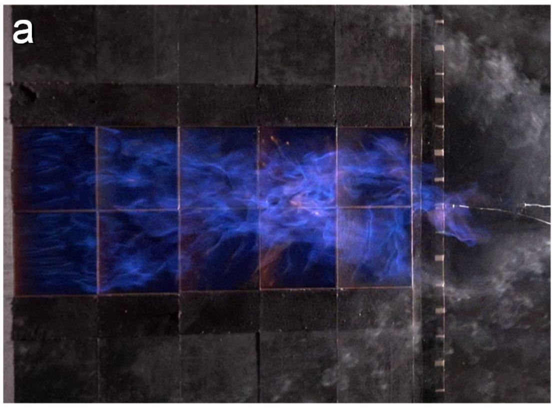

Figure 7. The flame shape, which indicates that the wind at both sides of the flame near the floor entered both sides of the flame. The wind direction was parallel to the long axis of the fuel pools.

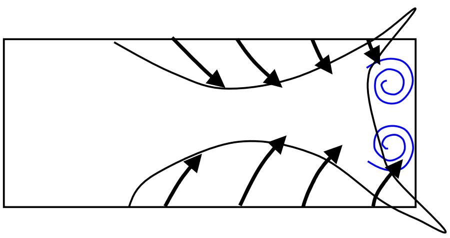

Figure 8. Schematic diagram showing the airflow entering the flame when the wind direction was parallel to the long axis of the fuel pools.

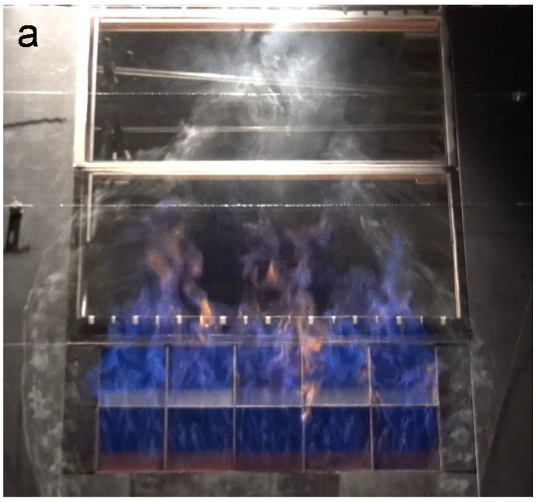

Figure 9. The flow around the flame when the wind direction was perpendicular to the long axis of the fuel pools. Smoke was injected 3 cm above the floor.

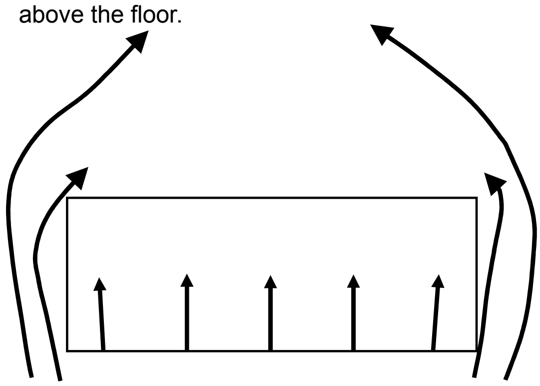

Figure 10. Schematic diagram showing the airflow around the flame when the wind direction was perpendicular to the long axis of the fuel pools. Lines passing both sides of the fuel pools were path (trajectory) of the smoke ejected 3 cm above the floor.

3.3 *The Effect of CVP on the Updraft in Fire Whirls*

CVPs may affect the updraft in fire whirls. We placed a smoke wire 80 cm above the floor upwind of the fire source. As shown in Figure 11(e) and (f), the view from beneath the glass plate reveals that smoke flowed toward the center from both sides and rose at the center toward the upwind direction. Figure 11(b) clearly shows that the smoke flowed toward the upwind direction. Figure 12 shows a view from the downwind of the flow. These figures clearly show that this flow downwind of the flame was due to a CVP and the upward flow between two vortices constituting the CVP flowed toward the upwind direction. Fire whirls were shed through the central region of the flow field, as shown in Figure 2(b). Figure 13 shows a side view of a fire whirl, and Figure 14 shows the vertical profile of wind velocity measured on the windward side of the fire source under no-flame conditions. Despite this wind profile, the fire whirl shown in Figure 13 was inclined toward the upwind direction. These results suggest that the updraft in fire whirls is affected by the rotation of CVPs.

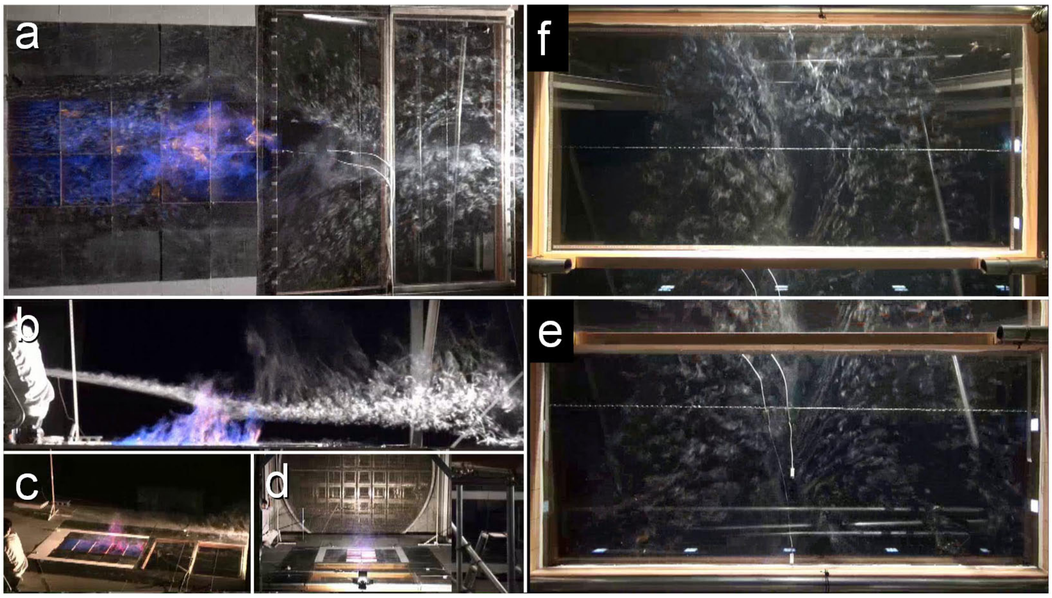

Figure 11. Images captured using the video cameras labeled a–f in Figure1. The wind direction was parallel to the long axis of the fuel pools and smoke was injected 80 cm above the floor upwind of the fire source.

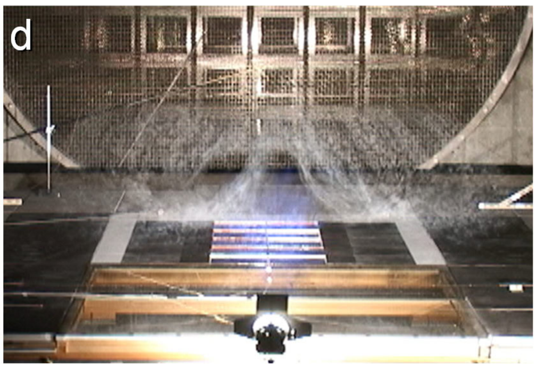

Figure 12. View from the downwind of the flow. The wind direction was parallel to the long axis of the fuel pools. Smoke was injected 80 cm above the floor upwind of the fire source.

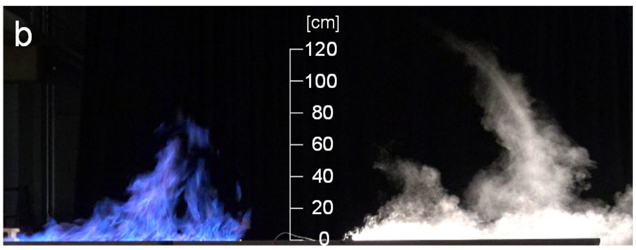

Figure 13. Side view of a fire whirl. Smoke was injected 3 cm above the floor downwind of the fire source.

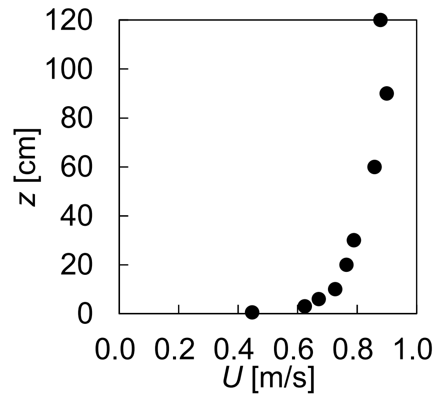

Figure 14. Vertical profile of the wind velocity measured on the windward side of the fire source under no-flame conditions.

3.4 *Discussion on Fire Whirls Behavior*

Here, we discuss the reason for the differences in the behavior of fire whirls in response to different wind directions. We estimate the balance between the downwind component of the wind velocity $U \sin\theta$, the velocity of air entrainment into the flame U_{ent}, and the velocity induced by another vortex constituting a vortex pair U_{ind}, as shown in Figure 15. Here, θ is the angle between the wind direction near the vortex and the *y*-axis. We did not considered U_{ind} when wind direction was parallel to the long axis of the fire source, as the direction of U_{ind} was *y*-axis direction because vortices were shed downwind one by one.

Table 1 lists the air entrainment velocity into each side of the fire source under no-wind conditions measured using the anemometer. Table 2 lists the temperature measured at the same location. These data were obtained during the period from when the flame covered all fuel pools until when the condition finished. The ambient temperature at the same location was 14.2°C when the fuel was ignited. Table 1 shows that entrainment velocity into the long side of the fire source U_{ent1} is larger than the velocity into the short side U_{ent2}. The difference between T_1 and T_2 also shows the effects of the width of the fire source on the environment around the flame.

Because we used the value of U_{ind} at x = 70 cm in the following discussion, we measured the value of U_{ent1} and U_{ent2} based on the motion of the smoke. When the wind direction was perpendicular to the long axis of the fire source, U_{ent1} ranged from 0.4 to 0.5 m/s at 40 ≤ x ≤ 100 cm. This is approximately equal to U_{ent1}, as listed in Table 1. When the wind direction was parallel to the long axis of the fire source, U_{ent2} was 0.4 m/s for x = 40 cm, 0.3 m/s for x = 70 cm, and 0.08 m/s for x = 100 cm. At x = 40 cm, U_{ent2} was equal to the value of U_{ent2} listed in Table 1. Therefore, we used 0.4 ≤ U_{ent1} ≤ 0.5 m/s and U_{ent2} = 0.3 m/s at x = 70 cm in further analyses.

To estimate the velocity U_{ind} induced by a vortex constituting a vortex pair, we assumed two straight vortex filaments of infinite length. The velocity induced by a straight vortex filament can be expressed as

$$U_{\mathrm{ind}} = \frac{K}{2\pi L}, \tag{1}$$

where K is the strength of a vortex filament, and L is distance between the centers of the vortices that constitute a vortex pair. K can be expressed as

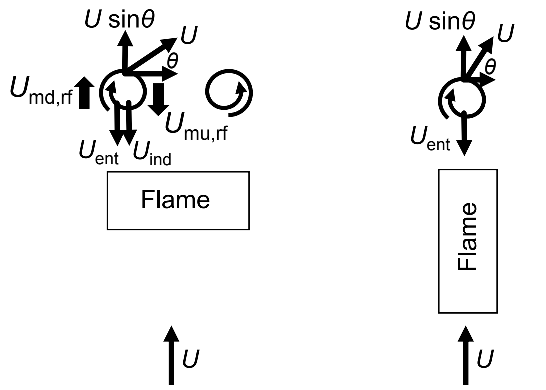

Figure 15. The velocities used in the discussion of the behavior of fire whirls.

Table 1. The entrainment velocities of air into each side of the fire source under no-wind conditions. Here U_{ent1} is the entrainment velocity into the long side of the fire source, and U_{ent2} is the entrainment velocity into the short side of the fire source.

	U_{ent1}	U_{ent2}	U_{ent1}/U_{ent2}
Mean [m/s]	0.52	0.42	1.22
Standard deviation (SD) [m/s]	0.10	0.08	1.22
SD/Mean [%]	18.3	18.3	1.00

Table 2. The Temperatures measured at the same location as the entrainment velocities listed in Table 1. Here T_1 is the temperature at the long side of the fire source, and T_2 is the temperature at the short side of the fire source.

	T_1	T_2
Mean [℃]	36.4	29.1
Standard deviation (SD) [℃]	6.3	4.8
SD/Mean [%]	17.3	16.4

$$K = 2\pi r_f U_{vor}\,, \tag{2}$$

where r_f is the radius of the forced vortex, and U_{vor} is the maximum velocity of the forced vortex (i.e., the velocity at r_f) under no-wind conditions. Because U_{vor} cannot be measured directly, we estimated it as follows. We assumed that maximum velocities in the vortex measured at both sides of the vortex (i.e., $U_{md,rf}$ and $U_{mu,rf}$ as shown in Figure 15) can be expressed as follows:

$$U_{md,rf} = U_{vor} + U\sin\theta - U_{ent} - U_{ind}, \tag{3}$$

$$U_{mu,rf} = U_{vor} - U\sin\theta + U_{ent} + U_{ind}, \tag{4}$$

where $U_{md,rf}$ is the maximum downwind velocity in the forced vortex, and $U_{mu,rf}$ is the maximum upwind velocity in the forced vortex. Using equations (3) and (4), U_{vor} is expressed as follows:

$$U_{vor} = \frac{(U_{md,rf} + U_{mu,rf})}{2}. \tag{5}$$

Figure 16 shows the distribution of downwind velocity in the horizontal plane in the vortices U_{md}, and Figure 17 shows the distribution of upwind velocity in the horizontal plane in the vortices U_{mu}. Based on these data, we obtained $U_{md,rf}$ = 1.4 m/s and $U_{mu,rf}$ = 1.0m/s at $r = r_f$ =0.1 m, where r is the distance from the center of vortices. Using these values and L = 0.4 m (see Figure 3(a)), we found U_{ind} = 0.3 m/s. Accurate measurements of the velocity fields are required to discuss the effects of the wind direction on velocity fields of the fire whirls.

We estimated U based on the motion of smoke at 70 < x < 90 cm, 50 < y < 80 cm and -80 < y < -60 cm, z = 3 cm. Locations far from the vortices were considered to reduce the effects of the vortices and entrainment into the flame. The angle θ was measured from streak lines generated by smoke from the wire.

Table 3 lists the results. When the wind direction was perpendicular to the long axis of the fuel pool, the total velocity of entrainment and the flow induced by another vortex was approximately equal to the downwind component of the wind, i.e., $U_{ent} + U_{ind} \approx U\sin\theta$. This is in agreement with the observation that the vortex pairs were almost stationary. When the wind direction was parallel to the long axis of the fuel pool, the estimated shedding velocity of the vortex ($U\sin\theta - U_{ent}$) was close to the measured velocity described in Section 3.1 (i.e., 0.5 m/s). These results suggest that the difference in the behavior of the fire whirls under different wind directions resulted from the strength of the entrainment into the flame and the velocity induced by the other vortex in the CVP.

We have previously measured the velocity

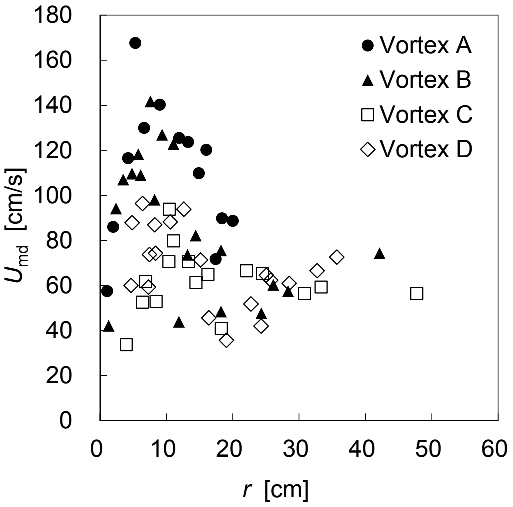

Figure 16. The distribution of the downwind velocity in the horizontal plane in the several fire whirls. Here r is the distance from the center of the vortices. With the vortices labeled A and B, the wind direction was perpendicular to the long axis of the fuel pools. With the vortices labeled C and D, the wind direction was parallel to the long axis of the fuel pools.

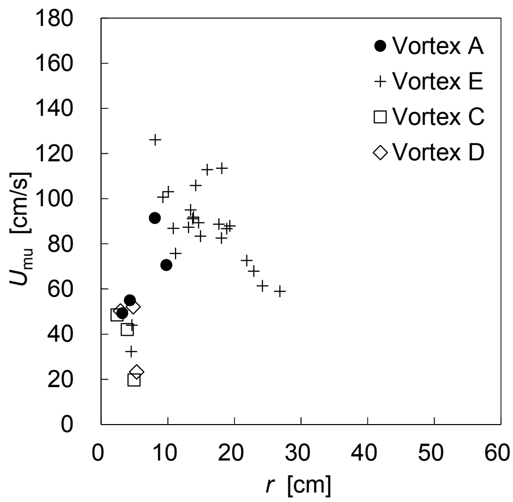

Figure 17. The distribution of the upwind velocity in the horizontal plane in the several fire whirls. Here r is the distance from the center of the vortices. With the vortices labeled A and E, the wind direction was perpendicular to the long axis of the fuel pools. With the vortices labeled C and D, the wind direction was parallel to the long axis of the fuel pools.

Table 3. The estimates used in the discussion of the behavior of fire whirls.

	θ [º]	$U\sin\theta$	U_{ent}	U_{ind}	$U_{ent}+U_{ind}$
Wind: perpendicular to the long axis of the fuel pools	45	0.6 – 0.9	0.4 – 0.5	0.3	0.7 – 0.8
Wind: parallel to the long axis of the fuel pools	60	0.65 – 0.85	0.3	–	0.3

fields downwind of the flame from a 30-mm-diameter burner using particle image velocimetry (PIV). The results (see Shinohara and Matsushima 2012, Fig. 7) showed that the wind appears to push only a part of a vortex downwind of the flame rather than the whole vortex. Therefore further observations and consideration are needed to describe this behavior fully.

4. CONCLUSIONS

We have described laboratory experiments to investigate the effects of the wind direction on the behavior of fire whirls occurring downwind of a 1.5 × 0.6-m rectangular fire source. We found that the behavior of fire whirls downwind of the rectangular fire source depended strongly on the wind direction.

The major results of this work can be summarized as follows.

(1) When the wind direction was perpendicular to the long axis of the fire source, the fire whirls formed vortex pairs that were almost stationary.

(2) When the wind direction was parallel to the long axis of the fire source, fire whirls were shed downwind one by one. We found that the updraft in the fire whirls appears to be affected by the rotation of CVPs in the plume from the flame. The formation process of the fire whirls was visualized. Vertical fire vortices appeared at the downwind side of the fire.

(3) When the wind direction was parallel to the long axis of the fire source, the motion of the smoke and the shape of the flame suggest that the wind at both sides of the flame near to the floor entered both sides of the flame. When wind direction was perpendicular to the long axis of the fire source, the wind near the floor appeared not to enter the sides of the flame.

(4) The entrainment velocity into the long side of the fire source was larger than that into the short side of the fire source under no-wind conditions.

REFERENCES

Cunningham, P., Goodrick, S. L, Hussaini, M. Y., and Linn, R. R., 2005: Coherent vortical structures in numerical simulations of buoyant plumes from wildland fires, *Int. J. of Wildland Fire* 14, 61–75.

Haines, D. A. Smith, M. C., 1983: Wind tunnel generation of horizontal roll vortices over a differentially heated surface, *Nature*, 306, 351-352.

Shinohara, M. and Kudo, K., 2004: Experimental Study of the Flow structure including whirlwinds in the wake region of a flame in a cross-wind, *Proc. of the 6th Asia-Oceania Symp. on Fire Science and Technology*, 120-131.

Shinohara, M., 2010: Formation of a counter-rotating vortex pair in a plume in a cross-flow, *Proc. of the 14th International Heat Transfer Conference, IHTC14-23283*. Washington, DC.

Shinohara, M., Matsushima, S., 2012: Formation of fire whirls: Experimental verification that a counter-rotating vortex pair is a possible origin of fire whirls, *Fire safety journal*, 54, 144-153.